PORT SAID ENGINEERING RESEARCH JOURNAL
Faculty of Engineering - Port Said University
Volume 27 No. 2 pp: 47 - 54

International Roughness Index Analysis of Paved Road using MLS Data

F.Ashraf[1], M. Rabah[2], and E. Ghanem[2]

[1] *Department of Civil Engineering, Higher Technological Institute, Tenth of Ramadan City, Egypt, email: fekry.ashraf@hti.edu.eg*

[2] *Department of Civil Engineering, Benha Faculty of Engineering, Benha University, Egypt, email: m.rabah@bhit.bu.edu.eg.,essam.ghanem@bhit.edu.eg.*

**Corresponding author,* *DOI: 10.21608/PSERJ.2023.187914.1215*

Received 20-1-2023
Revised 12-3-2023
Accepted 15-4-2023

ABSTRACT

Measuring the International Roughness Index (IRI) is a significant research field in developing intelligent transportation infrastructure systems. This study employed a mobile laser scanning (MLS) technique to measure the IRI from the standard deviation of longitudinal roughness (σ). The MLS technology provides a rapid and affordable alternative that produces precise and dense point clouds along route corridors. The IRI is often used as an indicator to assess the state of a pavement surface. Since the middle of the 20th century, several sensing technologies have been devoted to improving performance, functionality, and sensitivity. Using MLS, the IRI data were obtained from routes in Kuwait's Khiran city. The longitudinal sectors of the sections were extracted from the 3D point clouds collected by the MLS technique with a length of 2100 m. The longitudinal section was divided into the centerline, outer edge, and inner edge. The IRI was calculated every 100 m along the three longitudinal sections, and it was found that it changed from 4.9 mm to 19.3 mm for the centerline, from 7.9 mm to 41.9 mm for the outer edge, and from 6.2 mm to 35.4 mm for the inner edge. From the results, the general condition of the road is poor to very poor. There is excellent compatibility between the visual inspection of the road and the results from MLS data.

Keywords: International Roughness, Mobile Laser Scanner, Longitudinal Deviations.

1 INTRODUCTION

Pavement management systems (PMS) and surface pavement distress measurements have been utilized to analyze the state of the pavement at the network and project levels. The pavement condition index estimates the deterioration levels of road surface pavement based on cracking ratio, rutting depth, and the International Roughness Index (IRI). The pavement condition index serves as a tool to observe road conditions, plan for pavement maintenance, and develop upcoming rehabilitation processes. Previously, trained technicians or expert inspectors manually detected, identified, and classified pavement distresses. They would collect the required data by driving along the road at 5 to 10 km/h while using a clipboard or specialized keyboard of a PC acquisition device or by walking alongside the road and recording the pavement surface distresses using data forms. This manual technique has some limitations, including the inspectors' experience, the required time, high cost, low efficiency, the inability to cover all road sectors, and many risks [1].

The International Road Roughness Experiment (IRRE), conducted by research teams from numerous nations (Spain, the United States, Chile, and Brazil), established the IRI. Thus, it is known as the international roughness index. The IRI, which is determined using an athletic representation of a simulated quarter-car traveling to a measured profile at 80 km/h, is defined as a ratio of a vehicle's accumulated vertical suspension movement divided by the distance traveled [2]. Furthermore, a road meter mounted on a vehicle is used to obtain the measured profile [3]. IRI has gained popularity due to its stability and transferability worldwide, making it the most used road index globally [4]. As a result, ASTM and AASHTO suggest that the test section length be at least 0.1 miles for IRI determination [5&6].

Pavement roughness is calculated and represented using various global tools, techniques, and systems. These methods differ in technical difficulty, precision, price, and usage speed.

Globally, mobile laser scanning (MLS) has gained popularity as a form of surveying. This technology may collect data rapidly and accurately in large quantities. A point cloud with three-dimensional coordinates is the end product of MLS. It has several benefits, such as being less expensive and offering the information needed to create 3D models and topographic maps, detect road cracks, measure road width, and gradient, and create road cross-sections [7].

Point clouds from a street view are collected using MLS systems. These systems typically include an operational computer, digital cameras, a control unit, an inertial measurement unit (IMU), two GNSS antennas, a distance measurement instrument (DMI), and two laser scanners. The operating computer and the control unit are installed in a vehicle. The additional blocks are fixed to a platform on the vehicle's roof. Numerous companies, including Riegl Topcon, Leica, Optech, and Trimble, produce MLS systems. Each of these companies uses its software to process MLS data. The software's primary function is data adjustment and MLS system calibration. Between two laser scanners, relative orientation parameters are set during calibration. Multiple scans of the same scene and Ground Control Points (GCPs) are necessary for data adjustment. The absolute accuracy of MLS data adjustment relies on various elements, including the distance between the MLS system and a reference station. MLS system's technical specifications, the precision of GNSS measurements, the number of reference stations, and GCPs [8].

The type of scanned region affects the accuracy of GNSS measurements. For high-quality GNSS measurements, the absolute data accuracy for most MLS systems is 1 cm in both X, Y, and Z coordinates. It is essential to have an unobstructed view of the sky to receive strong GNSS signals. When GNSS signals are weak or lost, GCPs achieve absolute accuracy of 1 cm or better [9].

The pavement surface deviations from the designed surface grade are referred to as longitudinal pavement surface roughness. The vehicle dynamics, ride quality, and the effect of dynamic loads on the road surface are all impacted by these variances. The variation between the actual and theoretical surface road heights in a longitudinal section may take place due to road use, the construction process, or in some cases, a combination of both factors. For measured pavement profiles, statistics have been considered to represent the pavement surface roughness for longitudinal section. A statistic is a number that represents the variations in the pavement's surface [10].

2 THE ROAD CONDITION IN KUWAIT

In Kuwait, most road networks face numerous issues. It is annoying, distracting, and can cause a tragic accident. Various factors, such as a lack of a drainage system, axial loads, and a hot environment, frequently cause distress. Distresses such as surface treatment distresses, distortions, disintegration, cracking, and skid hazards can be categorized into different types [11].

3 LOCATION OF STUDY

The study was conducted in Al-Khiran Pearl City, Kuwait. The construction year before 2015 and the finish layer is flexible pavement .The Trimble MX2, a mobile mapping tool, was used to collect the point clouds for the study area. The accuracy of the technique used in this study is ± 1 cm and the range is up to 250 m. Figure 1 shows the Trimble MX2, figure 2 shows MLS point clouds for the road section, figures 3,5 show the road section from UAV data and figure 4 shows Al-Khiran Pearl City from UAV data.

Figure 1: Trimble MX2

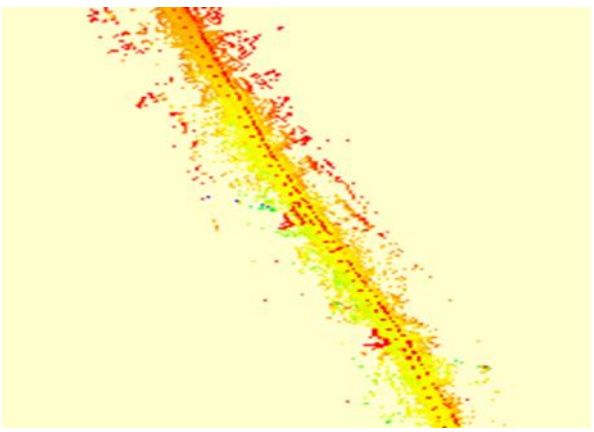

Figure 2: MLS point clouds for the road section

Figure 3: Road section

Figure 4: Study area from UAV data

Figure 5: Road section

4 RESULTS AND DISCUSSION

For the roughness analysis, the longitudinal sectors of the target sections were extracted from the 3D point clouds collected using MLS by dividing the road into three longitudinal sectors: the centerline, the outer edge, and the inner edge, with a length of 2100 m. The standard deviation of longitudinal roughness (σ) was calculated every 100 m along the road. Figure 6 shows the three longitudinal sectors, and Figure 7 shows the sections along the longitudinal section.

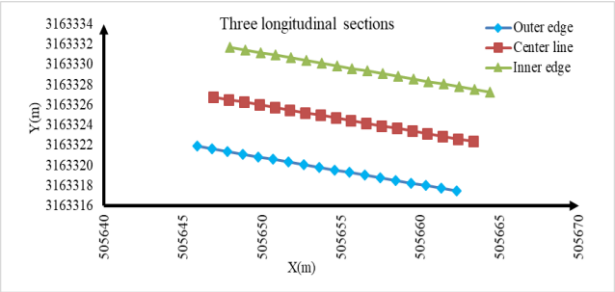

Figure 6: Three longitudinal sections for the longitudinal road section

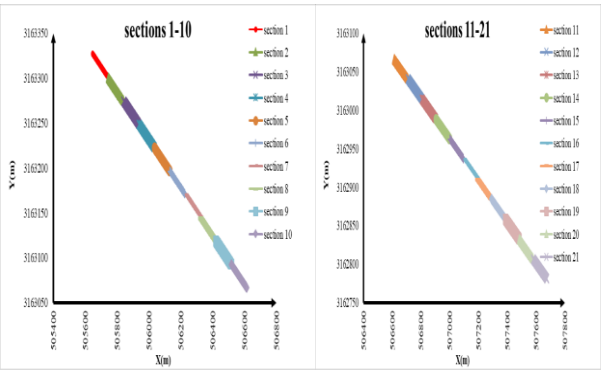

Figure 7: The sections along the longitudinal road section

The standard deviation of longitudinal roughness (σ) summarizes surface deviations. Hundreds of elevations were registered throughout the measurement, allowing the relative heights (di) to be calculated using the following equation (1):

$$d_i = h_i - \frac{1}{2}(h_{i-1} + h_{i+1}) \qquad \text{Eq. (1)}$$

Where d_i is the relative height and hi, hi-1, and hi+1 represent the registered surface elevations.

For pavement sections with a length of 100 m, a longitudinal roughness index (σ) can be calculated as the standard deviation of (di) values as follows:

$$\sigma = \sqrt{\frac{n_r \sum d_i^2 - (\sum d_i)^2}{n_r(n_r - 1)}} \qquad \text{Eq. (2)}$$

Where σ is the standard deviation or longitudinal roughness (in mm), d_i represents the reported profile heights, and n_r is the total number of registered data.

The IRI and σ values are statistically related based on the following equations:

$$IRI1 = 1.2054 \times \sigma + 0.1230 \quad R^2 = 0.92 \quad \text{Eq.(3)} \ [12].$$

$$IRI2 = 1.3068 \times \sigma + 0.0842 \quad R^2 = 0.93 \quad \text{Eq.(4)} \ [13].$$

Where σ represents the standard deviation of longitudinal roughness in mm and IRI is the international roughness index in mm/m.

Tables 1, 2, and 3 show the IRI results in mm/m from the standard deviation of longitudinal roughness (σ) in mm for the three longitudinal sections: centerline, outer edge, and inner edge, with lengths 2100 m every 100 m.

From Table 1, the standard deviation of longitudinal roughness (σ) of all sections along the longitudinal centerline sections varied from 4 mm to 18 mm, and the IRI1 and IRI2 varied from 4.9 mm/m to 19.7 mm/m, which indicated that the surface condition varied from poor to very poor condition.

Table 1: IRI for centerline section

Section	Stations		Centerline				
	Start	End	$\sum d_i$	$\sum di^2$	σ (mm)	IRI1 (mm/m)	IRI2 (mm/m)
1	0	0 + 100	1.075	0.033	15.0	18.2	19.7
2	0 + 101	0 + 200	0.706	0.008	5.0	6.2	6.6
3	0 + 201	0 + 300	1.033	0.043	18.0	21.8	23.6
4	0 + 301	0 + 400	0.463	0.003	4.0	4.9	5.3
5	0 + 401	0 + 500	0.769	0.009	5.0	6.2	6.6
6	0 + 501	0 + 600	0.625	0.006	4.0	4.9	5.3
7	0 + 601	0 + 700	1.009	0.016	8.0	9.8	10.5
8	0 + 701	0 + 800	1.003	0.020	10.0	12.2	13.2
9	0 + 801	0 + 900	0.632	0.006	5.0	6.2	6.6
10	0 + 901	1 + 00.0	1.414	0.031	11.0	13.4	14.5
11	1 + 00.0	1 + 100	1.499	0.031	9.0	11.0	11.8
12	1 + 101	1 + 200	1.043	0.015	7.0	8.6	9.2
13	1 + 201	1 + 300	1.371	0.028	10.0	12.2	13.2
14	1 + 301	1 + 400	1.484	0.039	13.0	15.8	17.1
15	1 + 401	1 + 500	0.659	0.008	6.0	7.4	7.9
16	1 + 501	1 + 600	1.027	0.016	8.0	9.8	10.5
17	1 + 601	1 + 700	1.611	0.039	11.0	13.4	14.5
18	1 + 701	1 + 800	1.329	0.027	10.0	12.2	13.2
19	1 + 801	1 + 900	1.526	0.038	12.0	14.6	15.8
20	1 + 901	2 + 0.00	1.535	0.034	10.0	12.2	13.2
21	2 + 00.0	2 + 100	1.385	0.028	10.0	12.2	13.2

From Table 2, the standard deviation of longitudinal roughness (σ) of all sections along the longitudinal outer edge sections varied from 6 mm to 32 mm, and the IRI1 and IRI2 varied from7.4 mm/m to 41.9 mm/m, which indicates that the surface condition varied from poor to very poor condition.

From Table 3, the standard deviation of longitudinal roughness (σ) of all sections along the longitudinal inner edge sections varied from 5 mm to 27 mm, and the IRI1 and IRI2 varied from 6.2 mm/m to 35.4 mm/m, which indicated that the surface condition varies from poor to very poor.

Table 2: IRI for the outer edge section

Section	Stations		Outer edge				
	Start	End	$\sum d_i$	$\sum di^2$	σ (mm)	IRI1 (mm/m)	IRI2 (mm/m)
1	0	0 + 100	2.449	0.162	32.0	38.7	41.9
2	0 + 101	0 + 200	1.089	0.043	18.0	21.8	23.6
3	0 + 201	0 + 300	0.833	0.011	7.0	8.6	9.2
4	0 + 301	0 + 400	0.920	0.018	10.0	12.2	13.2
5	0 + 401	0 + 500	1.056	0.017	8.0	9.8	10.5
6	0 + 501	0 + 600	0.928	0.015	8.0	9.8	10.5
7	0 + 601	0 + 700	0.831	0.011	6.0	7.4	7.9
8	0 + 701	0 + 800	0.839	0.011	6.0	7.4	7.9
9	0 + 801	0 + 900	1.152	0.022	9.0	11.0	11.8
10	0 + 901	1 + 00.0	1.189	0.029	12.0	14.6	15.8
11	1 + 00.0	1 + 100	1.536	0.043	14.0	17.0	18.4
12	1 + 101	1 + 200	1.141	0.019	8.0	9.8	10.5
13	1 + 201	1 + 300	1.873	0.135	32.0	38.7	41.9
14	1 + 301	1 + 400	1.211	0.024	10.0	12.2	13.2
15	1 + 401	1 + 500	1.314	0.064	22.0	26.6	28.8
16	1 + 501	1 + 600	1.450	0.055	19.0	23.0	24.9
17	1 + 601	1 + 700	1.589	0.054	17.0	20.6	22.3
18	1 + 701	1 + 800	1.617	0.051	16.0	19.4	21.0
19	1 + 801	1 + 900	1.645	0.047	14.0	17.0	18.4
20	1 + 901	2 + 0.00	1.813	0.048	12.0	14.6	15.8
21	2 + 00.0	2 + 100	1.505	0.047	16.0	19.4	21.0

Table 3: IRI for the inner edge section

Section	Stations		Inner edge				
	Start	End	$\sum d_i$	$\sum di^2$	σ (mm)	IRI1 (mm/m)	IRI2 (mm/m)
1	0	0 + 100	0.835	0.012694	8.0	9.8	10.5
2	0 + 101	0 + 200	0.950	0.016	8.0	9.8	10.5
3	0 + 201	0 + 300	0.642	0.007	5.0	6.2	6.6
4	0 + 301	0 + 400	0.723	0.012	8.0	9.8	10.5
5	0 + 401	0 + 500	0.804	0.016	10.0	12.2	13.2
6	0 + 501	0 + 600	0.863	0.012	6.0	7.4	7.9
7	0 + 601	0 + 700	1.688	0.046	13.0	15.8	17.1
8	0 + 701	0 + 800	1.303	0.034	13.0	15.8	17.1
9	0 + 801	0 + 900	0.838	0.011	6.0	7.4	7.9
10	0 + 901	1 + 00.0	2.407	0.091	18.0	21.8	23.6
11	1 + 00.0	1 + 100	2.843	0.120	20.0	24.2	26.2
12	1 + 101	1 + 200	2.172	0.072	16.0	19.4	21.0
13	1 + 201	1 + 300	1.895	0.063	17.0	20.6	22.3
14	1 + 301	1 + 400	2.936	0.142	24.0	29.1	31.4
15	1 + 401	1 + 500	1.875	0.054	14.0	17.0	18.4
16	1 + 501	1 + 600	2.500	0.102	20.0	24.2	26.2
17	1 + 601	1 + 700	3.354	0.172	24.0	29.1	31.4
18	1 + 701	1 + 800	3.360	0.180	26.0	31.5	34.1
19	1 + 801	1 + 900	3.365	0.187	27.0	32.7	35.4
20	1 + 901	2 + 0.00	2.582	0.102	19.0	23.0	24.9
21	2 + 00.0	2 + 100	3.238	0.163	24.0	29.1	31.4

Figure 8 shows IRI (mm/m) from the start station section (0 + 100.00) to the end station section (2 + 100.00) for the centerline longitudinal section. The IRI was found to change from 4.90 mm/m to 21.2 mm/m (equation 3) and from 5.30 mm/m to 23.6 mm/m (equation 4).

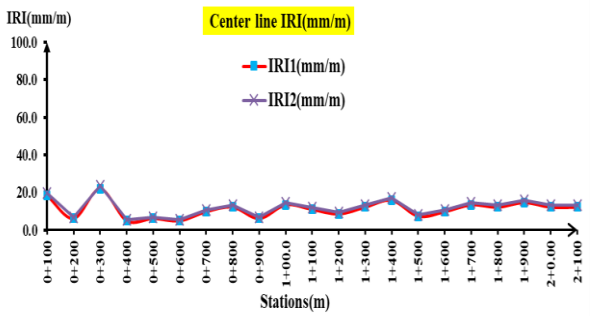

Figure 8: IRI for centerline longitudinal section

Figure 9 shows IRI (mm/m) from the start station section (0 + 100.00) to the end station section (2 + 100.00) for the outer edge longitudinal section. The IRI was found to change from 7.40 mm/m to 38.7 mm/m (equation 3) and from 7.90 mm/m to 41.9 mm/m (equation 4).

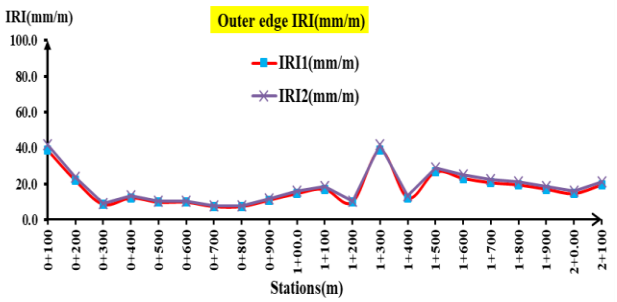

Figure 9: IRI for the outer edge longitudinal section

Figure 10 shows IRI (mm/m) from the start station section (0 + 100.00) to the end station section (2 + 100.00) for the inner edge longitudinal section. The IRI was found to change from 6.20 mm/m to 32.7 mm/m (equation 3) and from 6.60 mm/m to 35.4 mm/m (equation 4).

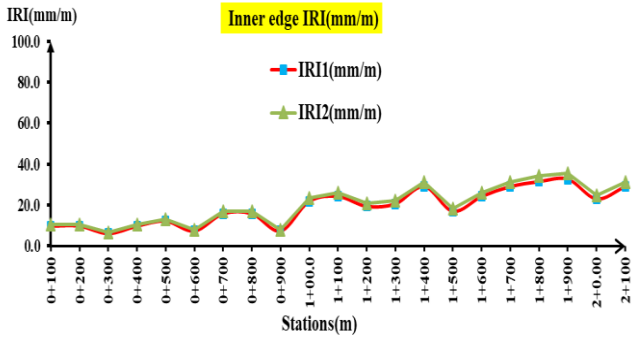

Figure 10: IRI for the inner edge longitudinal section

4.1 Prediction of the association between the present serviceability rating and IRI

A PSR-IRI relationship was developed using the PSR and IRI data for modeling and validation. PSR values were considered dependent, but IRI values were taken as independent variables. The present serviceability rating (PSR) of the road was estimated according to IRI results. The PSR for flexible pavement type ranged from 0 to 5 (very poor to very good), as defined in Table 4.

Table 4: The PSR ranges

0-1	1-2	2-3	3-4	4-5
Very poor	Poor	Fair	Good	Very good

Table 5 shows that the PSR values declined, and the IRI values increased as pavement conditions deteriorated. The correlation (R) between IRI and PSR= 0.973. The PSR for all sections varied from 2.1 to 0, indicating poor road surface conditions.

Table 5: PSR and IRI

IRI (mm/m)	4.9	6.2	7.4	8.6	9.8	11	12.2	13.4	14.6	15.8	18.2
PSR	2.1	1.8	1.5	1.2	0.9	0.7	0.5	0.4	0.2	0.1	0.0

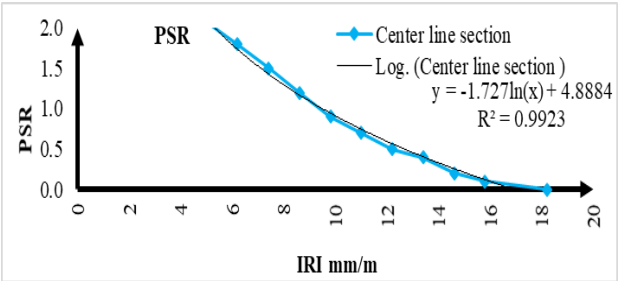

Figure 11: PSR and IRI for the road section

As presented in Figure 11, plots were drawn between the measured IRI and predicted PSR of the validation data with a view to validation. Therefore, the model can be utilized to estimate PSR from IRI for flexible pavement.

CONCLUSION

This study presented an MLS technique to measure the IRI from the standard deviation of longitudinal roughness (σ). The results showed that IRI changed from 4.9 mm to 19.3 mm for the centerline, from 7.9 mm to 41.9 mm for the outer edge, and from 6.2 mm to 35.4 mm for the inner edge. Based on the results, the general condition of the road is poor to very poor. Furthermore, there is significant compatibility between the visual inspection of the road and the results from MLS data. Therefore, the MLS technique can be used to study the road surface condition with high accuracy.

Author contributions

Essam Ghanem did the following:
(Project administration, Supervision, Final approval of the version to be published)

Mostafa Rabah did the following:
(Conception or design of the work, Data collection and tools, Data analysis and interpretation, Project administration, Supervision, Final approval of the version to be published)

Fekry Ashraf did the following:
(design of the work, Data collection and tools, Data analysis and interpretation, Funding acquisition, Resources, Methodology, Drafting the article, Critical revision of the article, Final approval of the version to be published)

Funding Statement:

No financial support was received.

Conflict of interest

The author declared that there are no potential conflicts of interest with regard to the research authorship or publication of this article.

REFERENCES

1. Imam R, Murad Y, Asi I, ·and Shatnawi A, "Predicting Pavement Condition Index from International Roughness Index using Gene Expression Programming," Innov. Infrastruct. Solut vol. 6 (3), 2021, pp. 1-12.
2. SAYERS M W. The little book of profiling: basic information about measuring and interpreting road profiles. University of Michigan, Ann Arbor, Transportation Research Institute, 1998.
3. SHAHIN M Y. Pavement management for airports, roads, and parking lots. 1994.
4. Zamora Alvarez, E J, Ferris, J B, Scott, D, and Horn, E. "Development of a discrete roughness index for longitudinal road profiles," Int. J. Pavement Eng, vol. 19(12), 2018, pp. 1043-1052.
5. AASHTO-R43. Standard Practice for quantifying roughness of pavements. American Association of State Highway and Transportation Officials, 2013.
6. ASTM-E867. Terminology Relating to Vehicle-Pavement Systems. American Society for Testing and Materials, 2002
7. Guan H, Li J, Yu Y, Wang C, Chapman M, Yang B, 2014. "Using mobile laser scanning data for automated extraction of road markings," ISPRS J. Photogramm. Remote Sens. Vol. 87, 2014, pp. 93–107.
8. Wang Y, Chen Q, Zhu Q, Liu L, Li C, and Zheng D, "A Survey of Mobile Laser Scanning Applications and Key Techniques over Urban Areas," Remote Sens, vol. 11(13), 2019, pp. 1540.
9. Altyntsev M A and Popov R A, "The Analysis of GPS Signal Short-term Loss Influence on the Accuracy of Mobile Laser Scanning Data". XXV FIG Congress, Malaysia, Kuala Lumpur, 16-21 June 2014.
10. Farias M M and Souza R O, "Longitudinal roughness and its influence on pavement functional evaluation." Proceedings VII National Meeting for Highways Conservation. CDROM. Vitória, Brazil. (In Portuguese), 2002.
11. AlKheder, S and AlKandari Y, "Mobile-based pavement system evaluation for Kuwait," Appl. Geomat, vol. 13.4, 2021, pp. 677-690.
12. PAIRC EVEN project, "The analysis performed on longitudinal profiles measured on in-service roads during the Permanent International Association of Road Congresses--World Road Association (PIARC) second international experiment, the EVEN project, which was conducted in the United States, Japan, and Europe in 1998".
13. Márcio M D and Ricardo O D, "Correlations and Analyses of Longitudinal Roughness Indices," June 2009.